

# Haptic Feedback with a Reservoir Computing-Based Recurrent Neural Network for Multiple Terrain Classification of a Walking Robot

Pongsiri Borijindakul<sup>1</sup>, Noparit Jinuntuya<sup>2</sup>, and Poramate Manoonpong<sup>1,3,\*</sup>

<sup>1</sup> Institute of Bio-inspired Structure and Surface Engineering,  
College of Mechanical and Electrical Engineering,  
Nanjing University of Aeronautics and Astronautics, Nanjing, China

<sup>2</sup> Department of Physics, Faculty of Science, Kasetsart University, Bangkok, Thailand

<sup>3</sup> CBR Embodied AI & Neurorobotics Lab, The MærskMc-Kinney Møller Institute,  
University of Southern Denmark, Odense M, Denmark

kobekang@nuaa.edu.cn, \*poma@nuaa.edu.cn

<http://neutron.manoonpong.com/>

**Abstract.** Terrain classification is an important feature for walking robots because it allows the robots to stably move and operate on the terrain. Different terrain classification techniques have been developed. The techniques include the use of different exteroceptive and proprioceptive sensors with different classification methods. Whereas these techniques have been widely used to classify flat, hard, and rough terrains, their application to soft terrains has not been fully addressed. Achieving soft-terrain classification will expand the operational range of walking robots. Thus, in this study, we propose a new technique to classify various terrains including soft ones. The technique exploits haptic feedback (expressed only through ground contact force measurement of a legged robot) and neurodynamics with the temporal memory of a reservoir computing-based recurrent neural network. We used six different terrains to evaluate the performance of the proposed technique. The terrains include sand (loose ground), foams with different softness levels (soft ground), and floor (hard ground). The experimental results show that we can successfully classify all terrains with an accuracy of above 70%. Furthermore, owing to the temporal memory of the network, if the haptic feedback is transiently missing, the network will be still be able to classify the terrain considerably well.

**Keywords:** Terrain classification · Soft terrains · Haptic feedback · Neural networks · Walking machines.

## 1 Introduction

Walking animals can stably move around and adapt their locomotion to the terrain. Walking robots, to achieve the same behavior, have to be able to differentiate terrain properties. Thus, terrain classification is an important feature

for robots. Different terrain classification techniques have been developed [1-10]. The techniques include the use of exteroceptive sensors (e.g., a camera [5], a 2D laser range finder [7]) and/or proprioceptive sensors (e.g., joint angles [11], tactile or ground contact force sensing [8-10], and a combination of joint motor current and ground contact force [12]) with different classification methods. The typical methods include the root-mean-square value [7], discriminant function [9], support vector machines [5,10], neural networks [13], and adaptive boosting machine learning [12]. These techniques, while impressive in their own right, have been used to mainly classify flat, hard, and rough terrains. Their application to soft terrain classification has not been fully addressed. Thus, in this study, we propose a new technique to classify various terrains including soft ones. Inspired by the work of [12,13], our technique exploits two main ingredients: i) haptic feedback (expressed only through ground contact force sensing [12]) and ii) neurodynamics with the temporal memory of a reservoir computing-based recurrent neural network [13]. Compared with the above-mentioned techniques, which typically require multiple proprioceptive sensors [12,13] or additional exteroceptive sensors [2-5], our approach here uses only a ground contact force sensor installed in a front leg of our hexapod walking robot. This sensor, or haptic feedback, provides a direct interaction between the leg and the terrain, thereby allowing the robot to sense different terrain softnesses which might be difficult to obtain by using an exteroceptive sensor. The feedback is directly processed through a recurrent neural network. Owing to the temporal memory of the network, if the feedback is transiently missing, the network will still be able to classify the terrain considerably well. We emphasize that the embedded temporal memory of the network leads to more robust classification compared to other techniques. Thus, our proposed technique can be a basis for expanding the operational range of walking robots to cover not only flat, hard, and rough terrains but also soft terrains.

## 2 Bio-inspired Hexapod Walking Robot System

In this study, we used our bio-inspired hexapod walking robot system to develop our terrain classification technique. The system consists of two main parts: (1) a bio-inspired robot hardware platform (AMOSII) and (2) neural locomotion control.

### 2.1 Bio-inspired Robot Hardware Platform

AMOS II (Fig. 1(a)) is a bio-inspired hexapod walking robot[10]. The morphology of cockroaches inspired the robot body. The robot has six identical legs that are connected to the truck. The truck consists of two thoracic jointed segments. AMOS II has in total 19 active joints (three at each leg and one backbone joint). Its active backbone joint is inspired by a cockroach. The backbone joint provides the flexibility to the body. In addition, the body joint torque is tripled by the use of gear to achieve a more powerful body joint motion. The thoracal-coxal (TC)

joint controls the forward/backward motion of the leg, the coxal-trochanteral (CTr) joint plays the role of extension and flexion of the second part of the leg, and the femoral-tibial (FTi) joint drives up/down motion of the third part of the leg. AMOSII also has six ground contact force sensors installed in its legs. In this study, we use only one ground contact force sensor at a front leg to receive haptic feedback for terrain classification.

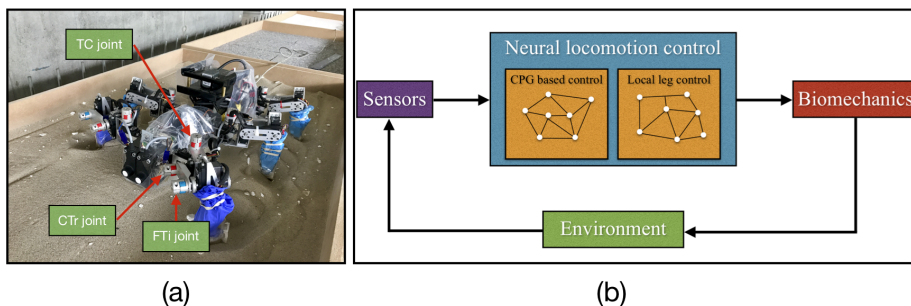


**Fig. 1.** (a) The bio-inspired robot hardware platform AMOSII. (b) Neural locomotion control of AMOSII.

## 2.2 Neural Locomotion Control

The locomotion control has been developed based on a modular structure. It consists of two main components: CPG-based control and local leg control [14] (Fig. 1(b)). The CPG-based control coordinates all leg joints of AMOS II, thereby generating insect-like leg movements and a multitude of different behavioral patterns. The patterns include forward/backward walking, turning left and right, and insect-like gaits. The local leg control using proprioceptive sensory feedback (such as ground contact force sensors) adapts the movement of an individual leg of AMOS II to deal with a change of terrain, loss of ground contact during the stance phase, or stepping on or hitting an obstacle during the swing phase. Each leg has two components facilitating local leg control: (1) an adaptive neural forward model, transforming the motor signal (efference copy) generated by the CPG into an expected sensory signal for estimating the walking state, and (2) elevation and searching control for adapting the leg motion (e.g., extension/flexion and elevation/depression). For more details of neural locomotion control, see [15].

## 3 Reservoir Computing-Based Recurrent Neural Network for Multiple Terrain Classification

Here we use the computational model using a recurrent neural network (RNN) of the reservoir computing (RC) type [16,17] (Fig. 2) for multiple terrain classification. Owing to the dynamic reservoir, the network with recurrent connections

exhibits a wide repertoire of nonlinear activity and temporal memory. Typically, the reservoir computing-based recurrent neural network has three layers: input, hidden, and output layers. The hidden layer is constructed as a random network with  $N$  hidden recurrent neurons and fixed randomly initialized synaptic connectivity.

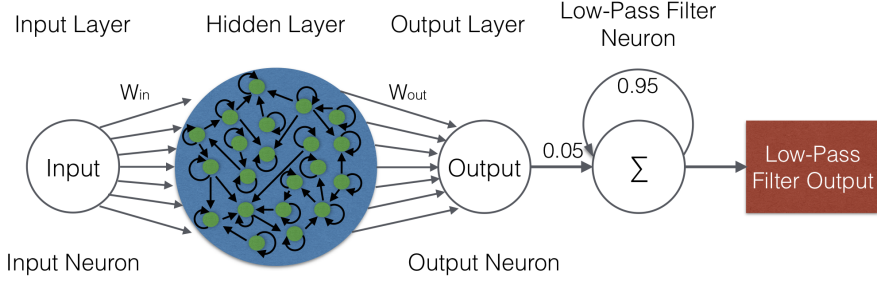


**Fig. 2.** Reservoir computing-based recurrent neural network for terrain classification.

The recurrent neural activity within the dynamic reservoir varies as a function of its previous activity and the current driving input signal. The discrete time state dynamics of reservoir neurons is given by:

$$\mathbf{x}(t+1) = (1 - \lambda)\mathbf{x}(t) + \lambda f_{sys}(\mathbf{W}_{in}\mathbf{u}(t+1) + \mathbf{W}_{sys}\mathbf{x}(t) + b_0), \quad (1)$$

$$y(t) = \mathbf{W}_{out}\mathbf{x}(t), \quad (2)$$

where  $\mathbf{x}(t)$  is the  $N$ -dimensional vector of neural state activations;  $\mathbf{u}(t)$  is the input to the reservoir, which, in this case, is a single CTr-motor signal (see Fig. 1(a));  $y(t)$  is the vector of output neurons. In this study, we use one output neuron to classify different terrains. The reservoir time scale is controlled by the parameter  $\lambda$ , where  $0 < \lambda \leq 1$ . Here the parameter is set to 0.9. A constant bias  $b_0 = 0.001$  is applied to the reservoir neurons.  $\mathbf{W}_{in}$  and  $\mathbf{W}_{sys}$  are the input to reservoir weights and the internal reservoir recurrent connection weights, respectively. The output weights  $\mathbf{W}_{out}$  are calculated using the recursive least squares (RLS) algorithm [18] at each time step, while the training input  $\mathbf{u}(t)$  is being fed into the network.  $\mathbf{W}_{out}$  are calculated such that the overall error is minimized. We implement the RLS algorithm using a fixed forgetting factor ( $\lambda_{RLS} < 1$ ) as follows:

$$e(t) = d(t) - y(t), \quad (3)$$

$$\mathbf{K}(t) = \frac{p(t-1)\mathbf{x}(t)}{\lambda_{RLS} + \mathbf{x}^T p(t-1)\mathbf{x}(t)}, \quad (4)$$

$$\mathbf{p}(t) = \frac{1}{\lambda_{RLS}} [\mathbf{p}(t-1) - K(t)\mathbf{X}^T(t)\mathbf{p}(t-1)], \quad (5)$$

$$\mathbf{W}_{out}(t) = \mathbf{W}_{out}(t-1) + K(t)e(t). \quad (6)$$

Here for each input set  $\mathbf{u}(t)$ , the reservoir state  $\mathbf{x}(t)$  and network output  $y(t)$  are calculated using Equations 1 and 2;  $e(t)$  is the error calculated from the difference between the desired output  $d(t)$  (here, foot contact signal) and the network output  $y(t)$ .  $K(t)$  is the RLS gain vector and  $\mathbf{p}(t)$  is the auto-correlation matrix updated at each time step. The reservoir to output weights  $\mathbf{W}_{out}$  are initially set to zero. The forgetting factor  $\lambda_{RLS}$  is set to a value less than 1 (here, we use 0.99). The auto-correlation matrix  $\mathbf{p}$  is initialized as  $\mathbf{p}(0) = \mathbf{I}/\beta$ , where  $\mathbf{I}$  is unit matrix and  $\beta$  is a small constant (i.e.,  $10^{-4}$ ). Details of all the fixed parameters and initial settings for the reservoir model are summarized in (Table 1). The network output  $y(t)$  is finally sent to a low-pass filter neuron (i.e., a single recurrent neuron with a linear transfer function, see Fig. 2) in order to smooth the output signal. Here we set the connection weight from the output neuron to the low-pass filter neuron to 0.05 while the recurrent weight of the low-pass filter neuron is set to 0.95.

**Table 1.** List of network parameter settings.

Parameter	Value
Number of input neurons	1
Number of output neurons	1
Number of hidden neurons	50
Learning mode	RLS
Internal transfer function ( $f_{sys}$ )	Tanh
Output transfer function	Linear
Input sparsity	20
Internal sparsity	50
Forgetting factor ( $\lambda_{RLS}$ )	0.99

RSL = the recursive least squares algorithm

Figure 3 shows the input, low-pass filter output, desired output, and error of the network. Figure 4 shows that the network can still predict the terrain although the network input which a foot contact sensor feedback is missing. Due to the temporal memory of the network, it allows the network to deal with the missing input information.

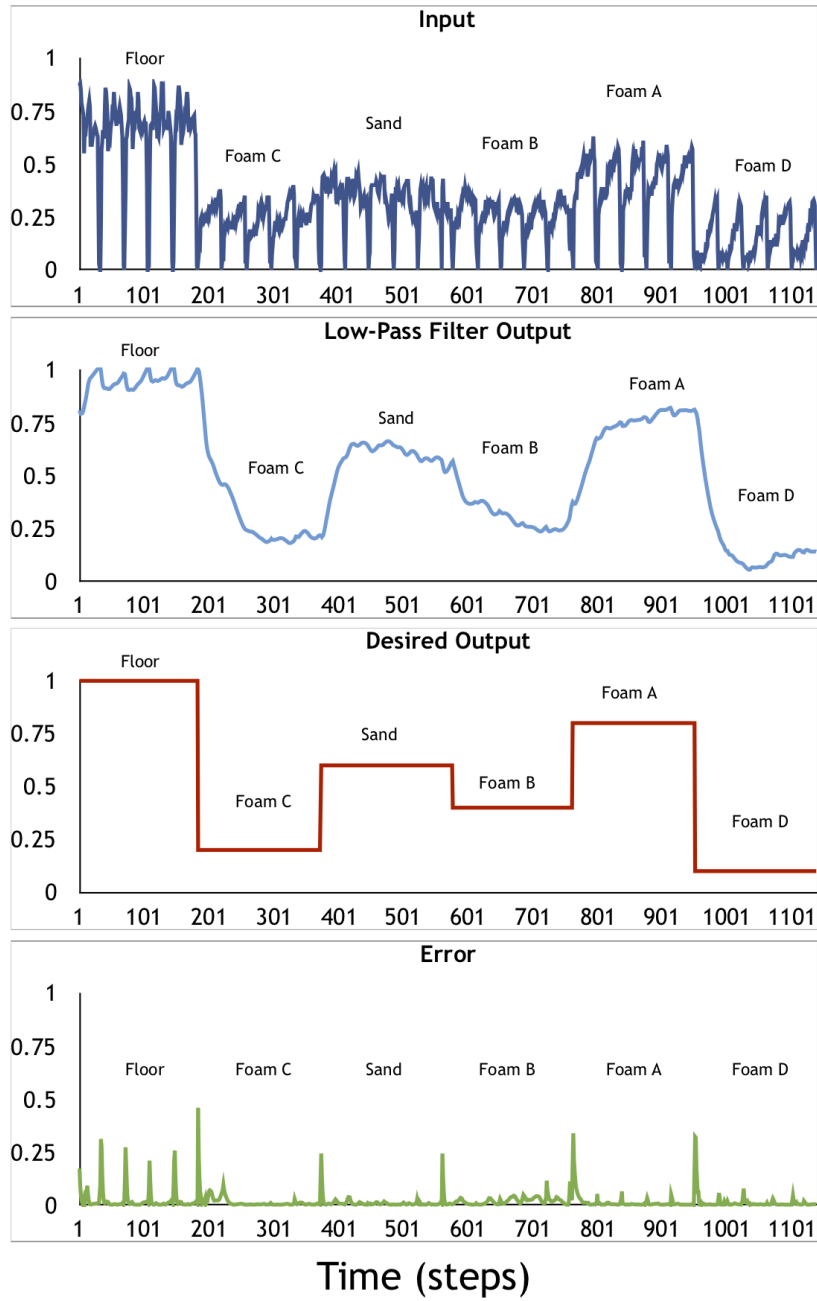


**Fig. 3.** Signals while the robot walked on different terrains. The first row shows the haptic feedback. The second row shows the output of the network. The third row shows the desired output and the last row shows the error between the desired output and the low-pass filter output.

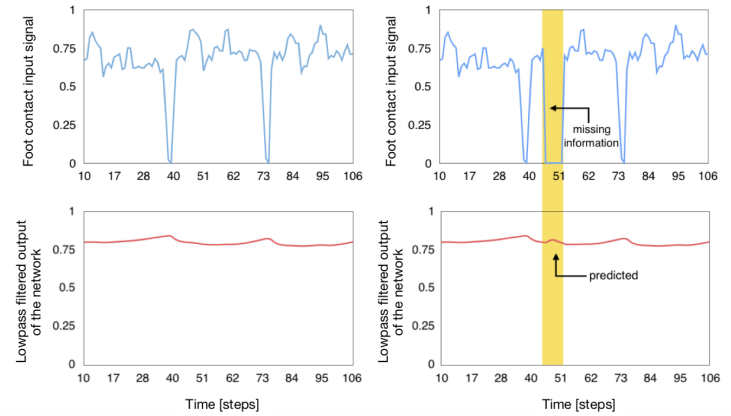


**Fig. 4.** An example of the prediction of lost information while the robot walked on the floor.

## 4 Multiple Terrain Classification

In our experiment, we chose six different terrains with different stiffnesses namely, floor, sand, foam of density  $80 \text{ kg/m}^3$  (foam A), foam of density  $32 \text{ kg/m}^3$  (foam B), foam of density  $89 \text{ kg/m}^3$  (foam C), and foam of density  $37 \text{ kg/m}^3$  (foam D) (see Fig. 5). First, we let the robot walk on the six terrains with a tetrapod gait and used the feedback from the foot contact sensor in the right front leg to indicate the terrain property. Figure 6 shows an example of the foot contact sensor feedback from the six terrains.

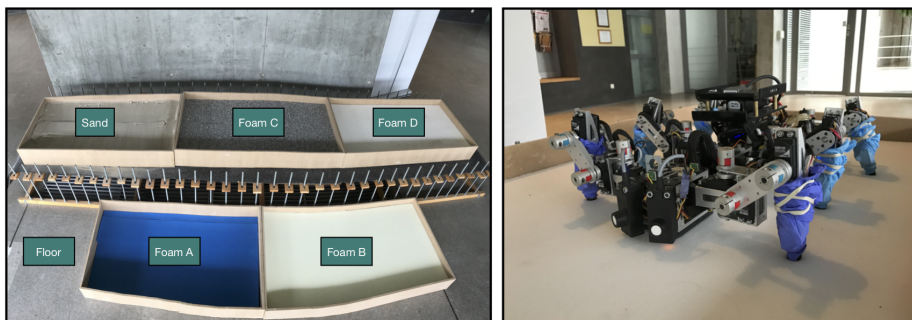


**Fig. 5.** Six different terrains for testing. The terrains include sand (loose ground), four foams with four different softness levels (soft ground), and floor (hard ground).

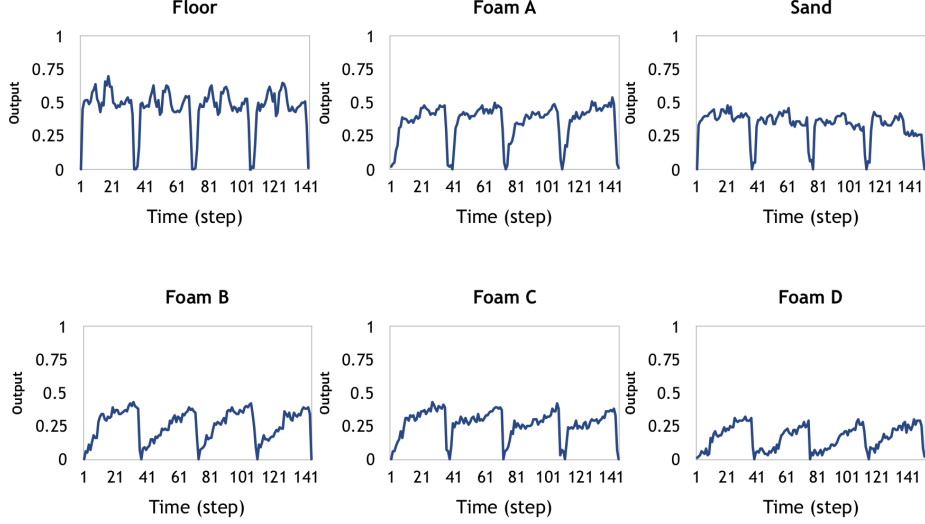


**Fig. 6.** Haptic feedback from the ground contact force sensor of the right front leg of AMOSII. The feedback was recorded while the robot walked on each terrain.

We applied force feedback from the robot leg to classify terrains by using our proposed reservoir computing-based recurrent neural network technique and compared with two different techniques, which are standard mean value and metrology techniques. The standard mean value technique is the widely used technique for analyzing data by using standard deviation. The standard deviation is a measure of how spread out numbers are and is calculated as the square root of the variance. Variance is the average of the squared difference from the mean. If  $y$  is the average value of force feedback on each terrain and  $Y$  is the outcome, then the results of force feedback are analyzed by using the standard deviation of testing values (see Equations 7 and 8):

$$Y = y \pm SD \quad (7)$$

$$SD = \sqrt{\frac{(x - \bar{x})^2}{n - 1}} \quad (8)$$

The metrology technique provides a high level of accuracy of data analyzed by using the expanded uncertainty. We evaluated the value of the repeatability of the measurement process to calculate the expanded uncertainty. Expanded uncertainty is the product of combined standard measurement uncertainty and a factor larger than 1. The expanded uncertainty ( $U$ ) is calculated as  $U =$  coverage factor  $k$  times combined uncertainty  $U_c(y)$  (see Equation 10), where  $k$

is from effective degrees of freedom. The effective degrees of freedom  $V_{eff}$  can be calculated from Equation 11, where  $c_i$  is the sensitivity coefficients,  $u(x_i)$  is the type A standard uncertainty,  $V_i$  is the degrees of freedom of  $u(x_i)$ , and  $N$  is the series of observations (here,  $N = 1$ ). For combined uncertainty in this work, we calculated only type A uncertainty (calculated from independent repeated observations( $n$ )) (see Equation 13) and set type B uncertainty (evaluated using available information) to zero because the sensor has good repeatability. We demonstrated the correction of classification through the confusion matrix (Table 2).

$$Y = y \pm U \quad (9)$$

$$U = kU_c(y) \quad (10)$$

$$k = V_{eff} = \frac{U_c^A(y)}{\sum_{i=1}^N \frac{c_i^A u^A(x_i)}{V_i}} \quad (11)$$

$$U_c = \sqrt{U_A^2 + U_B^2} \quad (12)$$

$$U_A = \frac{SD}{\sqrt{n}} \quad (13)$$

## 5 Experimental Results

Our experimental results show that the reservoir computing technique can be used to classify all types of terrains. The standard mean value technique can be used to classify only three terrains, which are foam A, foam D, and sand. This is because the average values of foam B and foam C are quite similar. The metrology technique can be used to classify only four terrains, which are foam A, foam B, foam D, and sand, whereas foam C cannot be unclassified. The standard mean value and metrology techniques both have a high percentage of unknown values because of the overlap of the average values as shown in (Table 2). The accuracy of classification of floor for the standard mean value and metrology techniques is higher than that of the reservoir computing because the terrain is even and the hardness of the floor is obviously higher than others. Moreover, the standard mean value and the metrology techniques classify terrains by using the average of input data, but the reservoir computing use both average input data and the differences in the characteristic of amplitude, therefore, if the signal looks similar, sometimes it would affect to the classification. In contrast, on the rest terrains, the reservoir computing method has higher accuracy than standard mean value and metrology technique (Fig. 7).

**Table 2.** Confusion matrix of three different techniques for multiple terrain classification. The vertical axis represents the actuals and the horizontal axis represents the output of the classification in percentage.

Confusion Matrix of RC Technique							
Tetrapod	Floor	Foam C	Sand	Foam B	Foam A	Foam D	unknown
Floor	92	0	0	0	8	0	0
Foam C	0	72	0	20	0	8	0
Sand	0	0	84	0	16	0	0
Foam B	0	20	8	72	0	0	0
Foam A	0	0	20	0	80	0	0
Foam D	0	21	0	0	0	79	0

Confusion Matrix of SD Technique							
Tetrapod	Floor	Foam C	Sand	Foam B	Foam A	Foam D	unknown
Floor	100	0	0	0	0	0	0
Foam C	0	0	0	0	0	8	92
Sand	0	0	48	24	0	0	28
Foam B	0	8	0	4	0	0	88
Foam A	0	0	12	0	60	0	28
Foam D	0	0	12	0	0	60	28

Confusion Matrix of Metrology Technique							
Tetrapod	Floor	Foam C	Sand	Foam B	Foam A	Foam D	unknown
Floor	100	0	0	0	0	0	0
Foam C	0	0	0	4	0	20	76
Sand	0	0	48	24	0	0	28
Foam B	0	8	0	40	0	0	52
Foam A	0	0	12	0	60	0	28
Foam D	0	0	12	20	0	60	8

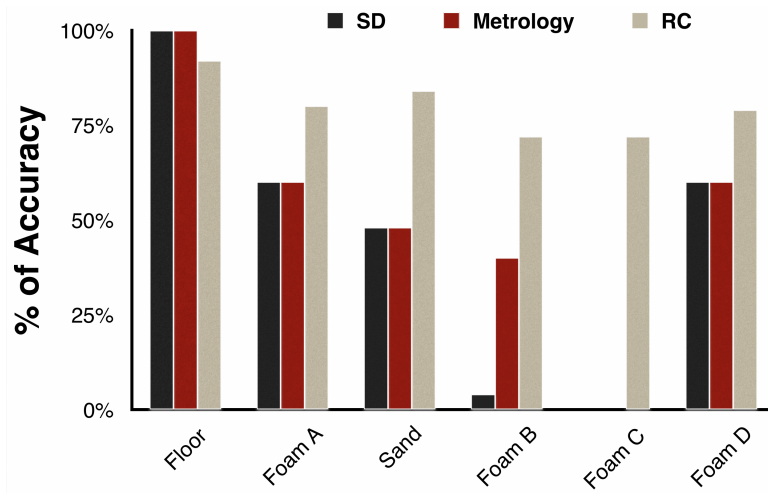


**Fig. 7.** The comparative accuracy chart of the three different methods on the six different terrains.

## 6 Conclusion

In this work, we demonstrated the performance of our reservoir computing-based recurrent neural network for multiple terrain classification by using haptic feedback. The reservoir computing technique can successfully classify all terrains with an accuracy of above 70% compared with the standard mean value and the metrology techniques, which cannot classify all terrains. Moreover, the proposed technique is also able to predict the missing or incomplete information while the robot walked and still can classify the terrain considerably well. In future work, we will implement ground contact force feedback from all legs to get more precise input data and complete terrain information to improve the terrain classification. We will also use the output of the classification method to allow the robot adapt its locomotion to the terrain.

## 7 Acknowledgments

This work was supported by the Capacity Building on Academic Competency of KU Students from Kasetsart University, Thailand, the Thousand Talents program of China, and the National Natural Science Foundation of China (Grant No. 51861135306).

## References

1. Williamson, D., Kottege, N., Moghadam, P.: Terrain Characterisation and Gait Adaptation by a Hexapod Robot. In: Australasian Conference on Robotics and Automation (ARAA). Brisbane, QLD, Australia (2016).
2. Stejskal, M., Mrva, J., Faigl, J.: Road Following with Blind Crawling Robot. In: International Conference on Robotics and Automation (ICRA). IEEE, pp. 3612–3617. Stockholm (2016). <https://doi.org/10.1109/ICRA.2016.7487544>
3. Krebs, A., Pradalier, C., Siegwart, R.: Comparison of Boosting based Terrain Classification using Proprioceptive and Exteroceptive Data. In: Khatib O., Kumar V., Pappas G.J. (eds) Experimental Robotics. Springer Tracts in Advanced Robotics, vol. 54, pp. 93–102. Springer, Berlin, Heidelberg (2008). [https://doi.org/10.1007/9783642001963\\_11](https://doi.org/10.1007/9783642001963_11)
4. Homberger, T., Bjelonic, M., Kottege, N., Borges, P. V. K.: Terrain-dependant Control of Hexapod Robots using Vision. In: Kulić D., Nakamura Y., Khatib O., Venture G. (eds) International Symposium on Experimental Robotics (ISER). Springer Proceedings in Advanced Robotics, vol 1, pp. 92–102. Springer, Cham (2017). [https://doi.org/10.1007/978-3-319-50115-4\\_9](https://doi.org/10.1007/978-3-319-50115-4_9)
5. Zenker, S., Aksoy, E. E., Goldschmidt, D., Wörgötter, F., Manoonpong, P.: Visual Terrain Classification for Selecting Energy Efficient Gaits of a Hexapod Robot. In: International Conference on Advanced Intelligent Mechatronics, IEEE/ASME, pp.577–584. Wollongong, NSW, Australia (2013). <https://doi.org/10.1109/AIM.2013.6584154>
6. Hoepflinger, M. A., Remy, C. D., Hutter, M., Spinello, L., Siegwart, R.: Haptic Terrain Classification for Legged Robots. In: International Conference on Robotics and Automation, IEEE, pp.577–584. Anchorage, AK, USA (2010). <https://doi.org/10.1109/ROBOT.2010.5509309>

7. Kesper, P., Grinke, E., Hesse, F., Wörgötter, F., Manoonpong, P.: Obstacle/Gap Detection and Terrain Classification of Walking Robots based on a 2D Laser Range Finder. In: 16th International Conference on Climbing and Walking Robots and the Support Technologies for Mobile Machines (CLAWAR), pp. 419–426. Australia (2013). [https://doi.org/10.1142/9789814525534\\_0053](https://doi.org/10.1142/9789814525534_0053)
8. Mrva, J., Faigl.: Tactile Sensing with Servo Drives Feedback only for Blind Hexapod Walking Robot. In: 10th International Workshop on Robot Motion and Control (RoMoCo), IEEE, Poznan, Poland (2015). <https://doi.org/10.1109/RoMoCo.2015.7219742>
9. Walas, K.: Tactile sensing for ground classification. *J. Autom. Mobile Robot. Intell. Syst* **7**(2), 18–23 (2013)
10. Wu, X.A., Huh, T.M., Mukherjee, R., Cutkosky, M.: Integrated ground reaction force sensing and terrain classification for small legged robots. *IEEE Robot. Autom. Lett* **1**(2), 1125–1132 (2016)
11. Best, G., Moghadam, P., Kottege, N., Kleeman, L.: Terrain classification using a hexapod robot. In: Guivant, J., Eaton, R. (eds) Proceedings of the Australasian Conference on Robotics and Automation (ACRA), pp.1–8. Sydney, Australia (2013)
12. Hoepflinger, M, A., Remy, C, D., Hutter, M., Spinello, L., Siegwart, R.: Haptic terrain classification for legged robots. In: 2010 IEEE International Conference on Robotics and Automation, IEEE, pp. 2828-2833. Anchorage, AK, USA (2010). <https://doi.org/10.1109/ROBOT.2010.5509309>
13. Jonas, D., Cauwenbergh R, V., Wyffels, F., Waegeman, T., Schrauwen B.: Terrain classification for a quadruped robot. In: 2013 12th International Conference on Machine Learning and Applications, IEEE, vol 1, pp. 185–190. Miami, FL, USA (2013). <https://doi.org/10.1109/ICMLA.2013.39>
14. Manoonpong, P., Parlitz, U., Wörgötter, F.: Neural Control and Adaptive Neural Forward Models for Insect-like, Energy-Efficient, and Adaptable Locomotion of Walking Machines. *Frontiers in Neural Circuits* **7**(12), 1–28 (2013)
15. Steingrube, S., Timme, M., Wörgötter, F., Manoonpong, P.: Self-organized adaptation of simple neural circuits enables complex robot behavior. *Nature Physics* **6**, 224–230 (2010)
16. Jaeger, H., Hass, H.: Harnessing nonlinearity: predicting chaotic systems and saving energy in wireless communication. *Science* **304**(5667), 78–80 (2004)
17. Dasgupta, S., Wörgötter, F., Manoonpong, P.: Information dynamics based self-adaptive reservoir for delay temporal memory tasks. *Evolving Systems* **4**(4), 235–249 (2013)
18. Jaeger, H.: Adaptive Nonlinear System Identification with Echo State Networks. In: *Advances in Neural Information Processing Systems*, pp.593–600. (2003)